Journal of Saudi Chemical Society (2017) **21**, S52–S57

King Saud University

**Journal of Saudi Chemical Society**

www.ksu.edu.sa
www.sciencedirect.com

ORIGINAL ARTICLE

# Adsorption characteristics of graphene oxide as a solid adsorbent for aniline removal from aqueous solutions: Kinetics, thermodynamics and mechanism studies

**Ali Fakhri** *

*Department of Chemistry, Shahre-Qods Branch, Islamic Azad University, Tehran, Iran*

Received 17 July 2013; revised 1 October 2013; accepted 3 October 2013
Available online 19 October 2013

**KEYWORDS**

Aniline;
Adorption;
Graphene oxide;
Isotherm;
Kinetics

**Abstract** The aim of this study is to investigate the possibility of graphene oxide (GO) as an alternative adsorbent for aniline removal from aqueous solution. Adsorption properties of GO for aniline removal were regularly investigated, including pH effect, adsorbent dose, temperature, contact time and initial concentration. The adsorption amount of aniline decreased with increasing pH. The experimental data were evaluated by Langmuir, Freundlich, Temkin and Harkins–Jura models in order to describe the equilibrium isotherms. Equilibrium data fitted well to the Langmuir model. The kinetic parameters achieved at different concentrations were analyzed using a pseudo first-order, pseudo second-order kinetic equation and intra-particle diffusion model. The experimental data fitted very well the pseudo second-order kinetic model. Thermodynamic parameters (free energy change, enthalpy change, and entropy change) announced that the removal of aniline from GO was endothermic and spontaneous. The study showed that GO could be used as an efficient adsorbent material for the adsorption of aniline from aqueous solution.


## 1. Introduction

The water is the most valuable natural resource, and because of its importance, it has become a dominant cause of concern. It has obtained more and more attention; the world became a foul with the maintenance and water purification. The petroleum refineries and the industries of plastics and paint are noxious sources for the sewage, which have the potential to destroy the receiving waters. Therefore, it is necessary to install convenience center for the treatment of the wastewater in places where these industries are posited.

Aniline is an important chemical compound which is well known for its abroad applications in the manufacture of dyestuffs, rubbers, pesticides, plastics and paints. However, the aniline-laden wastewater discharged from these industries has become a severe environmental difficulty as well. It is highly

* Tel./fax: +98 (21)22873079.
E-mail address: ali.fakhri88@yahoo.com.
Peer review under responsibility of King Saud University.

ELSEVIER Production and hosting by Elsevier

http://dx.doi.org/10.1016/j.jscs.2013.10.002

toxic and has adverse influences on human health and lentic life [10,4]. Moreover, aniline can be easily adsorbed in foulings, the fact that they can expand its insistence in the aquatic environment [24]. There are many processes, including biodegradation [21], oxidation by ozone [9], ligand exchanger [11], adsorption [30] and some other processes that can be used for the removal of aniline from wastewater. These processes can decompose or remove aniline from wastewater.

The adsorption phenomenon is probably the most widely employed manner in separation method [26], waste effluents treatment [23], refrigeration, environmental control and life support device in spacecraft, and obviously heterogeneous catalysis [8].

Graphene, a new carbon nanomaterial, has unique physical, chemical, electrical and mechanical properties [20,19,22,3] and is adequate for preparing nanodevices and advanced composite materials [2,27,25].

Recently, graphene and graphene oxide were used as adsorbents to remove methyl orange [14,15,16], naphthalene [31,32,33], 1-naphthol [31,32,33], arsenic [5], fluoride [14,15,16], heavy metals from aqueous solutions, and showed high adsorption amount and fast adsorption rates [6,7,29,31].

In this study, the removal characteristics of aniline were investigated using graphene oxide as the adsorbent. The adsorption isotherms and kinetics of the adsorbents were measured. The pH effect, adsorbent dose, temperature, contact time and initial concentration on aniline removal were also studied.

## 2. Materials and methods

### 2.1. Naive materials

Graphene oxide (GO) was prepared from natural graphite powder by the modified Hummers method [5]. A transmission electron microscopy (TEM, JEM-2100F HR, 200 kV) was used to characterize the size and shape of adsorbent. X-ray diffractometer (XRD) Philips X'Pert was used to characterize the adsorbent for its morphological information.

Aniline ($C_6H_5NH_2$) (molecular weight, 93.13 g/mol) was supplied by Merck, Germany (maximum available purity). Other chemicals, bought from Sigma Aldrich Co., Germany, are of analytical grade.

### 2.2. Batch experiments

Batch mode adsorption studies for aniline have been carried out to investigate the effect of different parameters such as adsorbate concentration, adsorbent dose, temperature and pH. Solution containing 20 mL adsorbate and 0.05 g adsorbent was taken in 250 mL capacity conical flask and agitated at 200 rpm in water bath shaker. The initial and final aniline concentrations remaining in solutions were analyzed by a UV spectrophotometer (Varian-Cary100 Bio), monitoring the absorbance changes at a wavelength of maximum absorbance $\lambda = 280$ nm. The equilibrium adsorption capacity was calculated from the relationship:

$$q(\mathrm{mg/g}) = \frac{(C_i - C)V}{C_i} \tag{1}$$

where $C_i$ and $C$ are the initial and residual concentrations of aniline in ppm, $q$ is the adsorption capacity in mg/g, $V$ is the volume of aniline solution in $L$, and $m$ is the adsorbent mass in $g$. The data analysis was carried out using correlation analysis employing least-square method and the residuals sum of square is calculated using the following equation [34]:

$$RSS = \sum \left[q_{e,\mathrm{exp}} - q_{e,\mathrm{cal}}\right]^2 \tag{2}$$

## 3. Results and discussions

### 3.1. Characterizations of graphene oxide

Fig. 1A shows the XRD patterns of GO. In the pattern of GO, the peak at $2u = 26.58$ was no longer detected and a new broader peak appeared at $2\theta = 11°$, demonstrated that the graphene structure with new oxygen containing groups was formed successfully by the strong oxidation reaction on the graphite.

The structure of GO was characterized by TEM and indicated in Fig. 1B. The TEM image of GO also corroborated that the GO existed in the sheet-like shapes. The BET analysis of the GO yielded a specific surface area of 305.8 $m^2\,g^{-1}$ [14,15,16].

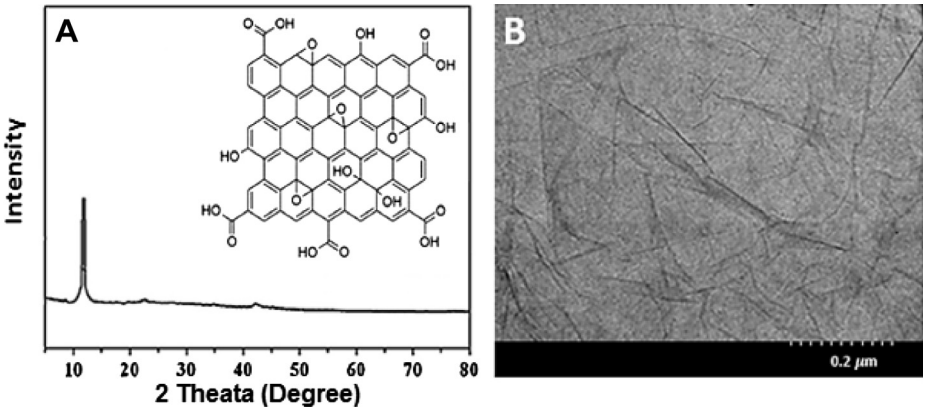


**Figure 1** XRD (A) and TEM (B) images of purified GO.

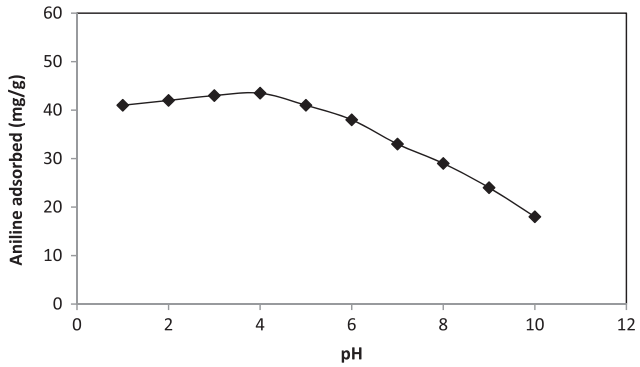


**Figure 2** Effect of pH value on aniline adsorption on GO ($C_0$ = 50 ppm, temperature 25 °C, adsorbent dosage 0.05 g, contact time 15 min).

### 3.2. Effect of pH on the adsorption capacity

To study the effect of pH on adsorption, experiments were carried out in the pH range 2–10 for aniline removal. Fig. 2 shows that the removal of aniline decreased with increasing initial pH of aniline solution and maximum value was reached at pH 4.0. As shown in Fig. 2, adsorption turnover of aniline is high and stable under acidic and neutral pH conditions and decreases with the increase of pH value under alkaline pH conditions. This trend may be explained on the basis of the fact that at low pH, aniline molecules readily enter into the pore structure of the common reed surface [18]. Lower adsorption of aniline at alkaline pH is likely due to the presence of excess $OH^-$ ions competing with aniline for the hydrogen bond formed with water molecules coordinated with GO in interlayer.

### 3.3. Effect of adsorbent dosage on the adsorption capacity

The results of experiments to distinguish the effects of adsorbent dosage on aniline removal are shown in Fig. 3 and reveal that the removal turnover of aniline by the GO increased with an increase in adsorbent dosage. While a prompt increase was observed at adsorbent dosages ranging between 0.01 and 0.05 g, a plateau was seen at those ranging between 0.05 and 0.11 g. Increasing of adsorbent dosage above 0.05 g had meager effect on the increase in removal efficiency of aniline. This

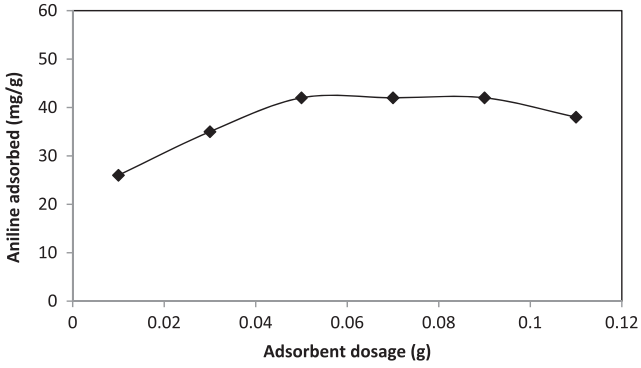


**Figure 3** Effect of the adsorbent dosage on aniline adsorption on GO ($C_0$ = 50 ppm, temperature 25 °C, pH 4, contact time 15 min).

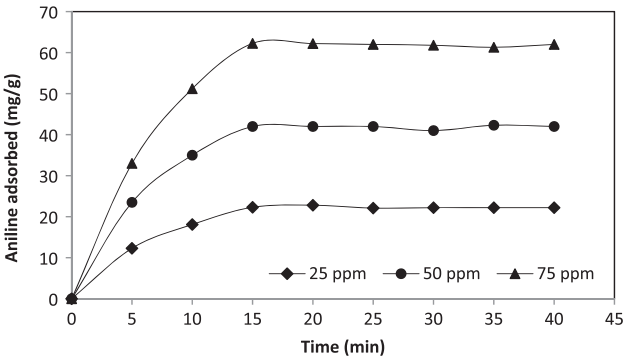


**Figure 4** Effect of contact time and initial concentration on aniline adsorption on GO (temperature 25 °C, adsorbent dosage 0.05 g, pH 4.0).

may be imputed to the formation of aggregates at higher solid/liquid ratios or to sediment of particles [1].

### 3.4. Effect of contact time and initial aniline concentration on the adsorption capacity

The effect of the initial aniline concentration on the removal rate onto GO at adsorbent dosage of 0.05 g is shown in Fig. 4. It can be seen that the adsorption at different concentrations is rapid in the initial stages and gently decreases with the improvement of adsorption until the equilibrium is attained. The amount of aniline adsorbed at equilibrium ($q_e$) increased as the initial concentration was increased. The initial concentration provides an important driving to overcome all mass transfer resistances of the aniline between the aqueous and solid phases. Hence, a higher initial concentration of aniline will enhance the sorption process. The aniline removal efficiency decreased as the aniline concentration was increased. Fig. 4 shows that the adsorption yield gradually increases with the extension of contact time and it remained constant after adsorption equilibrium was established at about 15 min.

### 3.5. Effect of temperature on the adsorption capacity

Temperature is an essential parameter for the study of adsorption, as the wastewater temperature varies widely. The effect of

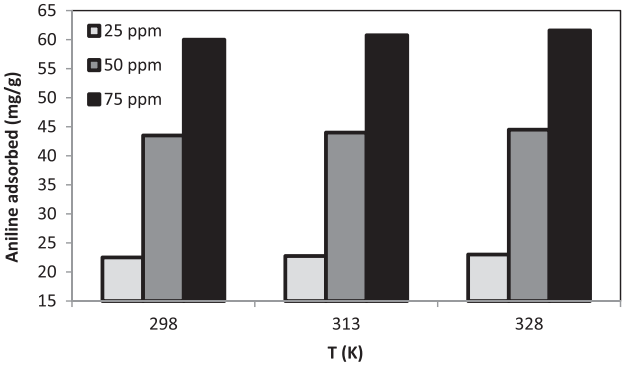


**Figure 5** Effect of temperature on aniline adsorption on GO (pH, 4.0; adsorbent dose, 0.05 g; contact time, 15 min).

temperature on the aniline uptake capacity of the adsorbent is presented in Fig. 5. The adsorption turnover increased with temperature increasing from 298 to 328 K, indicating the endothermic nature of the adsorption reaction of aniline onto GO. The increase of adsorption turnover with increased temperature indicated that the adsorption of aniline by GO might involve not only physical but also chemical sorption. This effect may be attributed to the increase in the number of adsorption sites generated due to bond rapture.

### 3.6. Adsorption isotherms

Equilibrium data, generally known as adsorption isotherms, are important in the basic design of adsorption systems, and are critical in optimizing the use of adsorbents. To optimize the design of an adsorption system for removing aniline from solutions, it is essential to establish the most appropriate correlation for the equilibrium curves. Several isotherm equations are available and four important isotherms are applied to fit the equilibrium data in this study: the Langmuir, Freundlich, Temkin, and Harkins–Jura isotherms are listed in Table 1.

The correlation coefficient ($R^2$) values of the four isotherms are also listed in Table 2. It could be consummated that the adsorption of aniline by GO, best fitted to the Langmuir isotherm equation. The fitness of the adsorption data to the Langmuir isotherm implies that the adsorption of aniline by GO is a multilayer adsorption applicable to heterogeneous surfaces. The applicability of the four isotherm's models for the present data nearly followed the order: Langmuir > Freundlich > Temkin > Harkins–Jura.

**Table 1** Summary of equilibrium isotherms ($K_L$, $K_F$, $B_1$, $K_T$, $A$, $B$: Langmuir, Freundlich, Temkin and Harkins–Jura constants; $n$: heterogeneity coefficient; $q_m$: maximum adsorption capacity; $q_e$: uptake at equilibrium; $C_e$: equilibrium concentration; $b$: activity coefficient related to mean sorption energy).

| Isotherm model | Equation |
|---|---|
| Langmuir | $\frac{C_e}{q_e} = \frac{1}{K_L q_m} + \frac{C_e}{q_m}$ |
| Freundlich | $\ln q_e = \ln K_F + \frac{1}{n}\ln C_e$ |
| Temkin | $q_e = B_1 \ln k K_T + B_1 \ln C_e$ |
| Harkins–Jura | $\frac{1}{q_e^2} = (\frac{B}{A}) - (\frac{1}{A}) log C_e$ |

**Table 2** Langmuir, Freundlich, Temkin and Harkins–Jura isotherm constants for adsorption of aniline.

| Isotherm | Temperature | | |
|---|---|---|---|
| | 298 K | 313 K | 328 K |
| *Langmuir* | | | |
| $q_m$ (mg/g) | 136.98 | 133.33 | 125.00 |
| $K_L$ (L/mg) | 0.0781 | 0.1038 | 0.1123 |
| $R_L$ | 0.3–0.6 | 0.3–0.6 | 0.3–0.6 |
| $R^2$ | 0.9969 | 0.9937 | 0.9923 |
| *Freundlich* | | | |
| $n$ | 1.443 | 1.472 | 1.506 |
| $K_F$ (mg/g) | 11.72 | 12.89 | 14.25 |
| $R^2$ | 0.9901 | 0.9899 | 0.9890 |
| *Temkin* | | | |
| $B_1$ | 26.216 | 25.984 | 25.668 |
| $K_T$ (L/mg) | 0.970 | 0.913 | 0.850 |
| $b = RT/B_1$ | 94.50 | 100.14 | 106.24 |
| $R^2$ | 0.9789 | 0.9771 | 0.9752 |
| *Harkins–Jura* | | | |
| $A$ | 344.82 | 370.37 | 400.00 |
| $B$ | 1.034 | 1.038 | 1.042 |
| $R^2$ | 0.9795 | 0.9725 | 0.9770 |

### 3.7. Adsorption kinetics

Several models can be used to prompt the mechanism of solute adsorption onto an adsorbent. In order to design a fast and effective model, investigations are made on adsorption rate. For the examination of the controlling mechanisms of adsorption process, such as chemical reaction, diffusion control and mass transfer, several kinetics models are used to test the experimental data.

#### 3.7.1. Pseudo-first-order kinetic model

The rate constant of aniline adsorption is distinctived by the pseudo-first-order kinetic model as proposed by [13]:

$$\ln(q_e - q_t) = \ln(q_e) - k_1 t \quad (3)$$

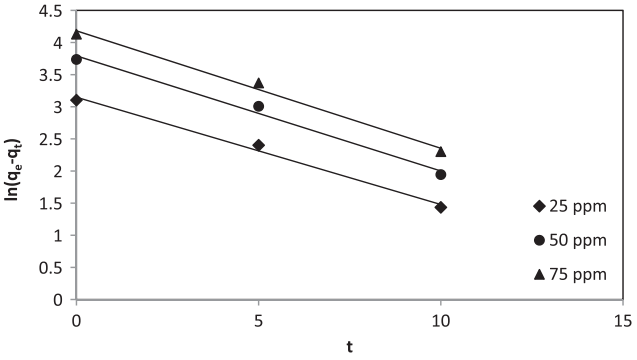


**Figure 6** Pseudo-first-order kinetic modeling of aniline adsorption on GO.

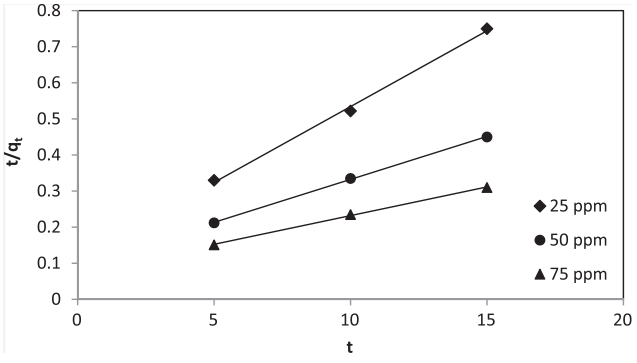


**Figure 7** Pseudo-second-order kinetic modeling of aniline adsorption on GO.

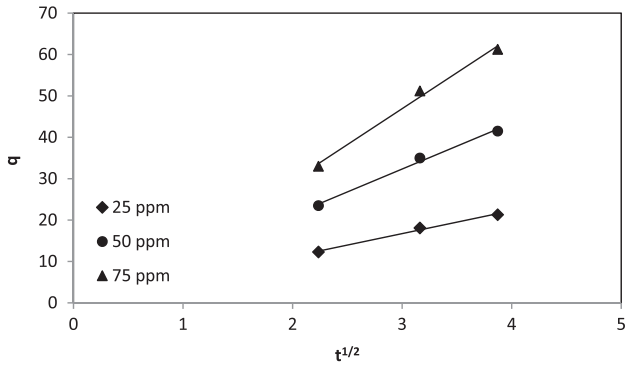


**Figure 8** Intra particle diffusion kinetic modeling of aniline adsorption on GO.

**Table 3** Constants of pseudo-first and second-order and intra-particle diffusion adsorption kinetic models.

| Kinetic model | Initial aniline concentration | | |
|---|---|---|---|
| | 25 ppm | 50 ppm | 75 ppm |
| $q_{experimental}$ | 22.3 | 42.00 | 62.25 |
| Pseudo-first-order | | | |
| $q_e$ (mg/g) | 24.29 | 44.37 | 65.47 |
| $k_1$ (1/min) | 0.1669 | 0.1792 | 0.1828 |
| $R^2$ | 0.9917 | 0.9886 | 0.9905 |
| RSS | 1.5 | 1.8 | 2.1 |
| *Pseudo-second-order* | | | |
| $q_e$ (mg/g) | 22.80 | 42.01 | 62.89 |
| $k_2$ (g /mg min) | 0.0168 | 0.0068 | 0.0034 |
| $R^2$ | 0.9976 | 0.9996 | 0.9989 |
| RSS | 0.3 | 0.1 | 0.3 |
| *Intra particle diffusion* | | | |
| $K_i$ (mg/g $min^{0.5}$) | 5.539 | 11.073 | 17.386 |
| $C$ | 0.1179 | 0.8810 | 5.2392 |
| $R^2$ | 0.9921 | 0.9931 | 0.9921 |
| RSS | 1.2 | 1.2 | 1.2 |

where $q_e$ and $q_t$ are the amounts of adsorbate adsorbed (mg/g) at equilibrium and at any instant of time $t$ (min), respectively, and $k_1$ is the rate constant of pseudo-first-order adsorption ($min^{-1}$). The values of $q_e$ and $k_1$ for the pseudo–first order kinetic model were determined from the intercepts and the slopes of the plots of ln $(q_e - q_t)$ *vs.* $t$ (Fig. 6), respectively.

### 3.7.2. Pseudo-second-order kinetic model

The pseudo-second-order kinetic model, based on equilibrium adsorption, can be demonstrated in the form [12]

$$\frac{t}{q_t} = \frac{1}{k_2 q_e^2} + \frac{t}{q_e} \tag{4}$$

where $k_2$ is the equilibrium rate constant of pseudo-second-order adsorption (g/(mg min)). A plot of $t/q_t$ *vs.* $t$ (Fig. 7) gives a linear relationship, from which $q_e$ and $k_1$ can be determined from the slope and intercept of the plot, respectively.

### 3.7.3. Intra-particle diffusion

The possibility of intra-particle diffusion resistance affecting adsorption was prospected by using the intra particle diffusion model as [28]:

$$q = k_i t^{1/2} + C \tag{5}$$

where $q$, $k_i$ and $C$ are the amount of aniline adsorbed (mg/g) at time $t$ (min), the intra particle diffusion rate constant (mg/g $min^{1/2}$) and the intercept, respectively (Fig. 8).Values of $C$ give an idea about the thickness of the boundary layer. According to this model, the plot of uptake should be linear if the intra particle diffusion is twisted in the adsorption process and if these lines pass through the origin then the intra particle diffusion is the rate controlling step [24].Furthermore the correlation coefficients ($R^2$) for the pseudo second-order kinetic model fits are 1.00, much higher than the correlation coefficients derived from other model fits (Table 3). Given the good agreement between model fit and experimentally observed equilibrium adsorption turnover in addition to the large correlation coefficients, it suggests that aniline adsorption followed pseudo second-order kinetics.

## 3.8. Thermodynamic parameters

The thermodynamic parameters such as Gibbs free energy change ($\Delta G^0$), enthalpy ($\Delta H^0$) and entropy ($\Delta S^0$) were computed using the following equations:

$$\Delta G^0 = -RT\ln K_c \tag{6}$$

$$\Delta G^0 = \Delta H^0 - T\Delta S^0 \tag{7}$$

where $K_C$ is the distribution constant for adsorption. The Gibb's free energy ($\Delta G^0$) for adsorption of aniline by GO obtained at all temperatures is listed in Table 4. $\Delta H^0$ and $\Delta S^0$ were determined from the slope and intercept of the plot of $\Delta G^0$ versus $T$ and are also tabulated in Table 4. The values of $\Delta G^0$ were negative at all temperatures and the negative values confirm the feasibility of the process and the spontaneous nature of aniline adsorption. The increase of the absolute value of $\Delta G^0$ as temperature rises indicates that the affinity of aniline on GO was higher at high temperature. The positive value of $\Delta H^0$ confirms that the adsorption reaction is endothermic. The positive value of $\Delta S^0$ reflects the affinity of the GO for aniline, and an increased randomness at the solid-solution interface during adsorption [17].

**Table 4** Thermodynamic parameters for the adsorption of aniline on GO.

| Initial aniline concentration | $\Delta H°$ (kJ $mol^{-1}$) | $\Delta S°$ (kJ $mol^{-1}$ $K^{-1}$) | $\Delta G°$ (kJ $mol^{-1}$) | | |
|---|---|---|---|---|---|
| | | | 298 K | 313 K | 328 K |
| 25 ppm | 6.564 | 0.040229 | −5.439 | −6.027 | −6.628 |
| 50 ppm | 5.092 | 0.032839 | −4.694 | −5.186 | −5.679 |
| 75 ppm | 3.484 | 0.023188 | −3.426 | −3.773 | −4.121 |

## 4. Conclusions

The aniline adsorption performance of GO was investigated in collectivity with adsorbent dosage, temperature and pH. Temperature and pH were found to have a great efficacy on the adsorption process. The strongest adsorption turnover was found in the solution at the acidic pH. Furthermore, the experimental data were best explained by the Langmuir isotherm model, and the adsorption kinetics of GO can be modeled successfully by pseudo-second-order rate equation. Thermodynamic parameters such as Gibbs free energy ($\Delta G$), enthalpy change ($\Delta H$) and entropy change ($\Delta S$) for aniline adsorption were found to be negative, positive, and positive, respectively. Therefore, the high adsorption turnover and excellent reusability demonstrate that GO has important potential as an adsorption material to remove aniline from aqueous solutions.

## Acknowledgment

The authors gratefully acknowledge the support of this research by the Islamic Azad University Shahre-Qods Branch.

## References

[1] J. Anandkumara, B. Mandal, Removal of Cr(VI) from aqueous solution using Bael fruit (*Aegle marmelos correa*) shell as an adsorbent, J. Hazard. Mater. 168 (2009) 633–640.
[2] P.K. Ang, W. Chen, A.T.S. Wee, K.P. Loh, Solution-gated epitaxial graphene as pH sensor, J. Am. Chem. Soc. 130 (2008) 14392–14393.
[3] A.A. Balandin, S. Ghosh, W. Bao, I. Calizo, D. Teweldebrhan, F. Miao, C.N. Lau, Superior thermal conductivity of single-layer graphene, Nano Lett. 8 (2008) 902–907.
[4] J.G. Cai, A. Li, H.Y. Shi, Z.H. Fei, C. Long, Q.X. Zhang, Adsorption characteristics of aniline and 4-methylaniline onto bifunctional polymeric adsorbent modified by sulfonic groups, J. Hazard. Mater. B124 (2005) 173–180.
[5] V. Chandra, J. Park, Y. Chun, J.W. Lee, I.C. Hwang, K.S. Kim, Water-dispersible magnetite-reduced graphene oxide composites for arsenic removal, ACS Nano 4 (2010) 3979–3986.
[6] V. Chandra, K.S. Kim, Highly selective adsorption of Hg2 + by a polypyrrole-reduced graphene oxide composite, Chem. Commun. 47 (2011) 3942–3944.
[7] X. Deng, L. Lü, H. Li, F. Luo, The adsorption properties of Pb(II) and Cd(II) on functionalized graphene prepared by electrolysis method, J. Hazard. Mater. 183 (2010) 923–930.
[8] F. Derbyshire, M. Jagtoyen, R. Andrews, A. Rao, I. Martin-Guillon, E.A. Grulke, Chem. Phys. Carbon 27 (2001) 1.
[9] P.C.C. Faria, J.J.M. Órfão, M.F.R. Pereira, Ozonation of aniline promoted by activated carbon, Chemosphere 67 (2007) 809–815.
[10] X. Gu, J. Zhou, A. Zhang, P. Wang, M. Xiao, G. Liu, Feasibility study of the treatment of aniline hypersaline wastewater with a combined adsorption/bioregeneration system, Desalination 227 (2008) 139–149.
[11] A.A. Gürten, S. Uc, M.A. Özler, A. Ayar, Removal of aniline from aqueous solution by PVC-CDAE ligand-exchanger, J. Hazard. Mater. 120 (2005) 81–87.
[12] Ho, Y.S., 1995. Adsorption of heavy metals from waste streams by peat, Ph.D. Thesis The University of Birmingham, Birmingham, UK.
[13] Lagergren S., 1898. Zur theorie der sogenannten adsorption gelöster stoffe, K. Sven, Vetenskapsakad. Handl, 24, 1–39.
[14] N. Li, M. Zheng, X. Chang, G. Ji, H. Lu, L. Xue, L. Pan, J. Cao, Preparation of magnetic CoFe2O4-functionalized graphene sheets via a facile hydrothermal method and their adsorption properties, J. Solid State Chem. 184 (2011) 953–958.
[15] Y.H. Li, P. Zhang, Q. Du, X. Peng, T. Liu, Z. Wang, Y. Xia, W. Zhang, K. Wang, H. Zhu, D. Wu, Adsorption of fluoride from aqueous solution by grapheme, J. Colloid. Interf. Sci. 363 (2011) 348–354.
[16] Y.H. Li, T. Liu, Q. Du, J. Sun, Y. Xia, Z. Wang, W. Zhang, K. Wang, H. Zhu, D. Wu, Adsorption of cationic red X-GRL from aqueous solutions by graphene: equilibrium, kinetics and thermodynamics study, Chem. Biochem. Eng. Q. 25 (2011) 483–491.
[17] Y. Liu, Y.J. Liu, Biosorption isotherms, kinetics and thermodynamics, Sep. Purif. Technol. 61 (2008) 229–242.
[18] K.S. Low, C.K. Lee, K.K. Tan, Bisorption of basic dyes by water hyacinth roots, Bioresour Technol. 52 (1995) 79–83.
[19] C.G. Navarro, M. Burghard, K. Kern, Elastic properties of chemically derived single graphene sheets, Nano Lett. 8 (2008) 2045–2049.
[20] K.S. Novoselov, A.K. Geim, S.V. Morozov, D. Jiang, Y. Zhang, S.V. Dubonos, I.V. Grigorieva, A.A. Firsov, Electric field effect in atomically thin carbon films, Science 306 (2004) 666–669.
[21] F. Orshansky, N. Narkis, Characteristics of organics removal by PACT simultaneous adsorption and biodegradation, Water Res. 31 (1997) 391–398.
[22] S. Park, K.S. Lee, G. Bozoklu, W. Cai, S.T. Nguyen, R.S. Ruoff, Graphene oxide papers modified by divalent ions—enhancing mechanical properties via chemical cross-linking, ACS Nano 3 (2008) 572–578.
[23] L.R. Radovic, C. Moreno-Catilla, J. Riveral-Utrilla, Chem. Phys. Carbon 27 (2000) 227.
[24] J. Sarasa, S. Cortes, P. Ormad, R. Gracia, J.L. Ovelleiro, Study of the aromatic byproducts formed from ozonation of anilines in aqueous solution, Water Res. 36 (2002) 3035–3044.
[25] S. Stankovich, D.A. Dikin, G.H.B. Dommett, K.M. Kohlhaas, E.J. Zimney, E.A. Stach, R.D. Piner, S.T. Nguyen, R.S. Ruoff, Graphene-based composite materials, Nature 442 (2006) 282–286.
[26] Y. Sudhakar, A.K. Dikshit, Removal mechanism of endosulfan sorption onto wood charcoal, Int. J. Environ. Poll. 15 (2001) 528–542.
[27] X. Wang, L. Zhi, K. Mullen, Transparent, conductive graphene electrodes for dye-sensitized solar cells, Nano Lett. 8 (2008) 323–327.
[28] W.J. Weber, J.C. Morris, Kinetics of adsorption on carbon from solution, J. Sanitary Eng. Div. Am. Soc. Civ. Eng. 89 (1963) 31–60.
[29] S.T. Yang, Y. Chang, H. Wang, G. Liu, S. Chen, Y. Wang, Y. Liu, A. Cao, Folding/aggregation of graphene oxide and its application in Cu2 + removal, J. Colloid Interf. Sci. 351 (2010) 122–127.
[30] J. Yao, X. Li, W. Qin, Computational design and synthesis of molecular imprinted polymers with high selectivity for removal of aniline from contaminated water, Anal. Chim. Acta 610 (2008) 282–288.
[31] N. Zhang, H. Qiu, Y. Si, W. Wang, J. Gao, Fabrication of highly porous biodegradable monoliths strengthened by graphene oxide and their adsorption of metal ions, Carbon 49 (2011) 827–837.
[32] G. Zhao, L. Jiang, Y. He, J. Li, H. Dong, X. Wang, W. Hu, Sulfonated graphene for persistent aromatic pollutant management, Adv. Mater. 23 (2011) 3959–3963.
[33] G. Zhao, J. Li, X. Wang, Kinetic and thermodynamic study of 1-naphthol adsorption from aqueous solution to sulfonated graphene nanosheets, Chem. Eng. J. 173 (2011) 185–190.
[34] M.H. Zwietering, I. Jongenburger, F.M. Rombouts, K.V. Riet, Modeling of bacterial growth curve, Appl. Environ. Microbiol. 56 (1990) 1875–1881.